

# Stacking Faults and Microstructural Parameters in Epoxy – Nylon Fabric – Clay Hybrid Laminates Using X –Ray Whole Powder Pattern Fitting Technique

Niranjana Prabhu<sup>1</sup>, Mahesh S S<sup>2</sup>, Nanda Prakash M B<sup>3</sup>, Demappa T<sup>4</sup>, Somashekar R<sup>3\*</sup>

<sup>1</sup>Department of Chemistry, East Point College of Engineering for Women, Bangalore, Karnataka, INDIA

<sup>2</sup>Department of Physics, Acharya Institute of Technology College, Bangalore, Karnataka, INDIA

<sup>3</sup>Department of Studies in Physics, University of Mysore, Manasagangotri, Mysore, Karnataka, INDIA

<sup>4</sup>Department of Studies in Polymer Science, Sir M.V. PG centre, Mandya, Karnataka, INDIA

**Abstract:** The changes in micro structural parameters in Epoxy – Nylon fabric laminates with 0.1 to 0.7 phr clay reinforcements have been studied using X-ray whole powder pattern fitting technique. The crystal imperfection parameters such as crystallite size  $\langle N \rangle$ , lattice strain (g in %) have been determined by line profile analysis (LPA) using Fourier method of Warren. Stacking faults ( $\alpha^d$ ) and twin faults ( $\beta$ ) are also determined by this method. The correlation index shows that there is a linear relationship between the stacking and twin fault density with crystallite size and it is observed that, the stacking and twin fault density increases with increase in average crystallite size. It is well known that the Fourier method gives a reliable set of micro structural parameters and we have shown that in addition to these values, one can also compute reliable fault probabilities which are very small in Epoxy – Nylon fabric laminates.

**Key Words:** Stacking faults ( $\alpha^d$ ) and Twin faults ( $\beta$ ), XRD, Crystallite size  $\langle N \rangle$ , Lattice strain (g in %), line profile analysis (LPA).

## I. INTRODUCTION

Fields such as waste containment facilities, flooring, agriculture sector, packaging, etc utilize various laminates in different form [1]. Polymers such as low density polyethylene (LDPE), medium density polyethylene (MDPE) and high density polyethylene (HDPE) are used in different packaging applications in the form of flexible films and laminates in pipe extrusion and injection molding of different items [2]. Carbon fabric reinforced polymeric composites are used for preparing flaps, aileron, and landing –gear doors [3]. HDPE film will be used as a linear material for its good strength, outstanding chemical resistance and minimal extractable matter [4]. The appropriate performance of these composites finds applications related to their mechanical properties and thermal resistance as a result of the adequate combination of reinforcement (tapes or fabrics), polymeric matrix and processing technique [5, 6].

Nylon – 66 Nano fabrics interleaving in epoxy/carbon fiber have shown improved impact resistance by 60% [7]. The epoxy resins (thermo set polymer type) used in aeronautical area, because they generally attend the mechanical strength, chemical resistance and service temperature requirements [8, 9]. The epoxy resin allows modifications in its chemical structure depending on the required application.

Line Profile Analysis, a powerful method to investigate the micro structural parameters like crystal size ( $\langle N \rangle$ ), lattice strain (g in %) and stacking faults in polymer materials [10–16] is used. Currently, several software packages which employ whole powder pattern fitting, to derive the micro structural parameters are commercially available [17–19]. Recently IUCr also conducted Round Robin test to evaluate the different procedures used to determine the crystallite size and lattice strain [20–22]. All these approaches, in principle, are based on multiple order method proposed by Warren and Averbach [14]. A majority of these methods employ a single distribution function for the whole pattern from which result an average set of micro structural parameters. Whole Powder Pattern Fitting Method et al [22] have also suggested a single-order method employing Voigt function and integral breadth of reactions. For polymers it is very rare to find experimentally, the multiple reflections. To overcome this inherent difficulty, a method employing simple, analytical asymmetric function [14] for individual size profile has been proposed in this synopsis. This method also enables the use of a single crystal size distribution function to account for the whole diffraction pattern which is adequate to quantify the stacking faults in materials like metal oxide compounds, but may be inadequate for describing diffraction patterns from polymers [24,25]. In this context, we would also like to emphasize that as per the Round Robin survey conducted by International Union of Crystallography (IUCr) [26], Fourier method of profile analysis (single order method used here) is quite reliable.

Here we discuss the method to compute crystallite size, lattice strain and stacking faults present in Epoxy – Nylon fabric laminates with 0.1 to 0.7 phr clay reinforcements have been studied using whole pattern fitting technique. Using the parameters computed from the single line analysis, the whole pattern observed in Epoxy – Nylon fabric laminates has been simulated. The extent of variation of these parameters obtained from single-order method while refining against the whole pattern refinement is also discussed.

### A. Experimental

Huntsman Araldite MY740 Epoxy Resin, K112 Accelerator and Aradur HY918 Hardener were obtained from Huntsman Advanced Materials Private Limited (Mumbai, India). Nylon interwoven fabric was obtained from Reliance Industries Limited (Mumbai, India). The fabric had the following morphological features: fibers in the fabric were of 50 mm diameter, 120 mesh, 145 mm fabric thickness and 62 g/m<sup>2</sup>. Cloisite 30-B clay was procured from Southern Clay products Inc. (Texas, USA). The average particle size as given by the supplier was 10 mm with a density of 1.98 g/cc. All the chemicals were used without any modifications.

Laminate hybrids of epoxy–nylon fabric (five layers) were prepared by incorporating clay particles as reinforcement with a loading of 0.1–0.7 phr using a conventional hand layup technique. Initially, clay was mixed with 100 phrepxy and stirred for 30 min at 1350 r/min using a conventional variable speed TANCO stirrer (PLT-184) (Tanko Screw products, IL, USA). Then, 2 phr accelerator and 85 phr hardener were mixed with the epoxy–clay mixture for another 5 min at 1350 r/min. The nylon interwoven fabrics of size 200 x 100 mm were dipped into the clay mixed epoxy and layered (five layers) between two Teflon release sheets and rolled. The samples were cured at 100°C for 2 h and postcured at 120°C for 4 h between two iron plates.

### B. The X-ray Diffraction Pattern

X-ray diffraction pattern of Epoxy – Nylon fabric laminates samples were recorded on Rigaku Miniflex II Diffractometer with Ni filtered, CuK<sub>α</sub> radiation of wavelength 1.542 Å, and a graphite monochromator. The scattered beam from the sample was focused on to a detector. The specifications used for the recording were 30 kV and 15 mA. The Epoxy – Nylon sample was scanned in the 2θ range of 6° to 60° with a scanning speed of 5° per min and step size of 0.02°. The X-ray scattering measurements were performed at the WAXS/SAXS beam line of the LNLS (Laboratorio Nacional de Luz Sincrotron-Campinas, Brazil), by using monochromatic beam of wavelength

1.7433 Å. The scattering intensity was registered using a one dimensional position-sensitive gas detector for a sample-detector distance of 1641.5 mm. The scan range (2θ) was 10° to 50°. WAXS curves were obtained from the WAXS images by band integration tool supplied by X-ray 1.0 software, produced by University Mons Hainaut.

### C. Electron Microscope Studies

In order to establish the dispersion characteristics of the prepared hybrid composites, the morphological features of the fractured surfaces of impact broken samples have been observed using scanning electron microscopy (SEM). The observed microscopic images revealed a good dispersion of clay particles at low clay loading (Figure 1(b) and (c)) and agglomeration build-up at higher clay loading (Figure 1(d) to (f)). In neat epoxy–nylon sample, the fiber pullout is relatively low compared with other samples (Figure 1(a)). However, fiber pullout perpendicular to the impact direction has increased with the increase in clay content. As the clay content increased beyond 0.2 phr, the agglomeration of clay particles has decreased the strength between the matrix and the fiber.

## II. THEORY

### A. X-Ray Diffraction Data Analysis:

The contribution of crystallite size, lattice strain and stacking faults to a Bragg reflection profile can be written as [14]

$$I_{hkl}(s_{hkl}) = \int_{-\infty}^{\infty} T^{IP}(nd) e^{[2\pi i \zeta(nd)]} e^{[2\pi i \phi(nd)]} e^{[2\pi i nd s_{hkl}]} d(nd) \quad (1)$$

where  $I_{hkl}(s_{hkl})$  is the intensity of a profile in the direction joining the origin to the center of the reflection,  $T^{IP}$  is the Fourier transform of instrument profile,  $e^{[2\pi i \zeta(nd)]}$  is the average phase factor due to lattice distortion ( $\zeta$ ) and  $e^{[2\pi i \phi(nd)]}$  is due to crystallite size / stacking faults ( $\phi$ ).  $L = nd$  (with  $d = d_{hkl}$ ) is the column length. For a detailed discussion on the equation used here to compute X-ray whole powder pattern, we refer to our earlier publications [27].

The whole powder pattern of samples were simulated using individual Bragg reflections represented by the above equations using

$$I(s) = \sum_{hkl} (\omega_{hkl} I_{hkl} - BG) \quad (2)$$

where  $\omega_{hkl}$  are the appropriate weight functions for the (hkl) Bragg reflection. Here  $s$  takes the whole range ( $2\theta \approx 6^\circ$  to  $60^\circ$ ) of X-ray diffraction recording of the sample. BG is an error parameter introduced to correct the background estimations.

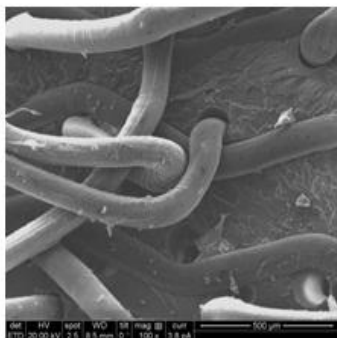


Figure 1(a)

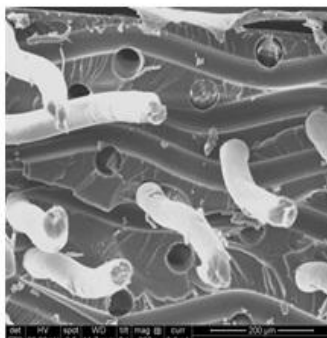


Figure 1(b)

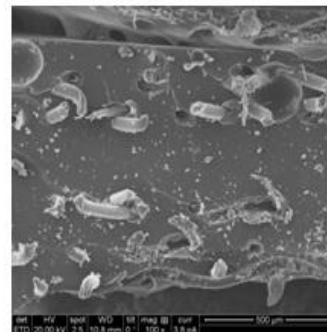


Figure 1(c)

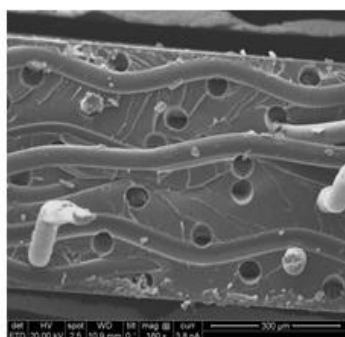


Figure 1(d)

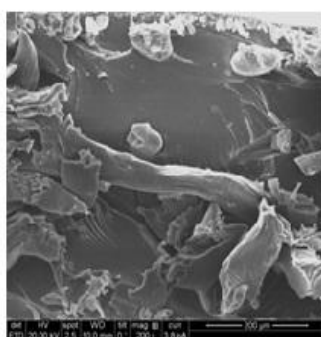


Figure 1(e)

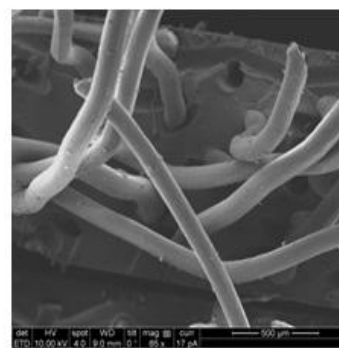


Figure 1(f)

**Figure 1:** (a) SEM of neat epoxy–nylon laminate. (b) SEM of epoxy–nylon–0.1 phr clay laminate. (c) SEM of epoxy–nylon–0.2 phr clay laminate. (d) SEM of epoxy–nylon–0.3 phr clay laminate. (e) SEM of epoxy–nylon–0.5 phr clay laminate. (f) SEM of epoxy–nylon–0.7 phr clay laminate.

### III. RESULTS AND DISCUSSION

In the first step, the micro structural parameters were refined for individual profiles of X-ray recordings in each of the sample and the computed values of crystallite size  $\langle N \rangle$ , lattice strain (g in %), stacking fault probability and twin fault probability are given in **Table 1** for Epoxy fabric laminates with 0.1 to 0.7 phr. **Figure 1(a-f)** shows the morphology of impact broken samples was investigated using an Environmental Scanning Electron Microscope, Quanto – 200, FEI, The Netherlands .We observe that the lattice strain in epoxy fabric laminates with 0.1 phr to 0.7 phr is 0.5% to 1% and average crystallite area increases from  $98.37 \text{ \AA}^2$  to  $171.9 \text{ \AA}^2$  as clay concentration increases from 0.1 phr to 0.7 phr. **Figure 2** shows simulated and experimental profiles for epoxy fabric laminates with 0.1 phr to 0.7 phr obtained with exponential column length distribution The standard deviations in all the cases for the micro structural parameters are given in **Table 1** as  $\Delta$ . This  $\Delta$  represents the statistical percentage of deviation of the parameters. The agreement between simulated and experimental intensity of the individual profiles in each of

the samples are less than 10% of the mean value. With these parameters given in **Table 1** as an input, we have further refined these parameters against the whole pattern ( $2\theta \approx 6^\circ$  to  $60^\circ$ ) recorded from the samples by taking summation which extends over the whole pattern [equation (7)]. We have observed small but significant changes in these parameters with the set convergence of 1%. These changes are also given in **Table 1**. The goodness of the fit between simulated and experimental profiles for the samples was given in **Figure 2**. The observed variation in the micro structural parameters given in **Table 1** is due to a two-fold refinement. First we have carried out the line profile analysis of the extracted profiles from overlapping regions, which is a standard procedure to compute the micro structural parameters. Secondly, the range of overlapping regions determines the extent of broadening of the reflections. In fact, the broadening may decrease if the reflections are closer together and hence results in an increase in the crystallite size values. A closer look at the results in **Table 1** and also the whole pattern indicates such a problem. It is worth noting that none of other parameters,

such as lattice strain and stacking fault probability, varied much during the refinement against the whole pattern data of the samples.

To check the reliability of the computed deformation and twin faults, we have used a simple approximate method suggested by Warren [15] and the expression for the twin fault is given by,

$$(2\theta_{CG}^0 - 2\theta_{PM}^0)_{hkl} = -14.6X_{hkl} \tan \theta \times \beta \quad (3)$$

where  $2\theta_{CG}^0$  is the center of gravity of the Bragg reflection profile and  $2\theta_{PM}^0$  is the peak maxima,  $\beta$  is the twin fault and  $X_{hkl}$  is the constant value, which we have taken to be 0.23. For all the samples we have computed the average twin fault probabilities are comparable to the values obtained by incorporating an appropriate expression in the Fourier coefficients. From this we would like to emphasize that these values are reliable and do represent the twin faults present in the sample in a direction perpendicular to the axis of sample. In fact,  $1/\beta$  represents the number of layers between two consecutive twin fault layers. We have also approximately estimated the deformation fault probability value  $\alpha^d$  by making use of the following expression given by Warren [15]

$$\frac{1}{\langle D_s \rangle} = \frac{1}{\langle D \rangle} + [(1.5\alpha^d + \beta) / d_{hkl}] \left[ \sum_b |L_0| / (u+b)h_0 \right] \quad (4)$$

where  $h_0 = (h^2 + k^2 + l^2)^{1/2}$ ,  $u$  is the un broadened component,  $b$  is the broadened component and  $L_0 = 3N+1$  reflections. A comparison with the deformation fault probability values obtained by Fourier coefficient method (**Table 1**) indicates that the values are low, because there are too many layers between two successive deformation fault layers. This is due to the fact that there are pockets of crystalline like order in a matrix of amorphous regions. It is well known that the Fourier method gives a reliable set of micro structural parameters and we have shown that in addition to these values, one can also compute reliable fault probabilities.

A graphical plot of the crystallite shape ellipse shown in **Figure 3** was obtained by taking the crystal size value

corresponding to  $2\theta \approx 17.69^\circ$  along the X-axis and the other parameter corresponding to  $2\theta \approx 29.09^\circ$  along the Y-axis for epoxy fabric laminates with 0.1 to 0.3 phr and 0.7 phr. These crystallite shape ellipsoid for the different samples the strength of the samples are normally proportional to crystalline area which is equal to ellipsoid area determined by micro structural parameters. It is evident that the crystallite shape ellipsoid area for epoxy fabric laminates with 0.1 phr to 0.7 phr increases with clay concentration. We have calculated the stacking probability of finding a hexagonal or cubic environment in the stacking arrangement, which are the parameters used in the early works of Jagodzinski [28,29] and these values are given in the Table 1. It is worth noting that none of other parameters, such as lattice strain and stacking fault probability, varied much during the refinement against the whole pattern data of the samples low, because there are too many layers between two successive deformation fault layers. This is due to the fact that there are pockets of crystalline like order in a matrix of amorphous regions. It is well known that the Fourier method gives a reliable set of micro structural parameters and we have shown that in addition to these values, one can also compute reliable fault probabilities. **Figure 4(a)** and **Figure 4(b)** shows the variation of stacking faults and Twin faults with crystallite size for Pure Epoxy – Nylon fabric laminates.

## CONCLUSION

Whole X - ray pattern fitting procedure developed by us has been used to compute micro crystalline parameters. The important aspect of this investigation is that crystalline area increases as clay concentration increases. We have studied the microcrystalline parameters from XRD. The correlation index shows that there is a linear relationship between the stacking and twin fault density with crystallite size and it is observed that, the stacking and twin fault density increases with increase in average crystallite size. This is due to the fact that there are pockets of crystalline like order in a matrix of amorphous regions. It is well known that the Fourier method gives a reliable set of micro structural parameters and we have shown that in addition to these values, one can also compute reliable fault probabilities which are very small in Epoxy – Nylon fabric laminates.

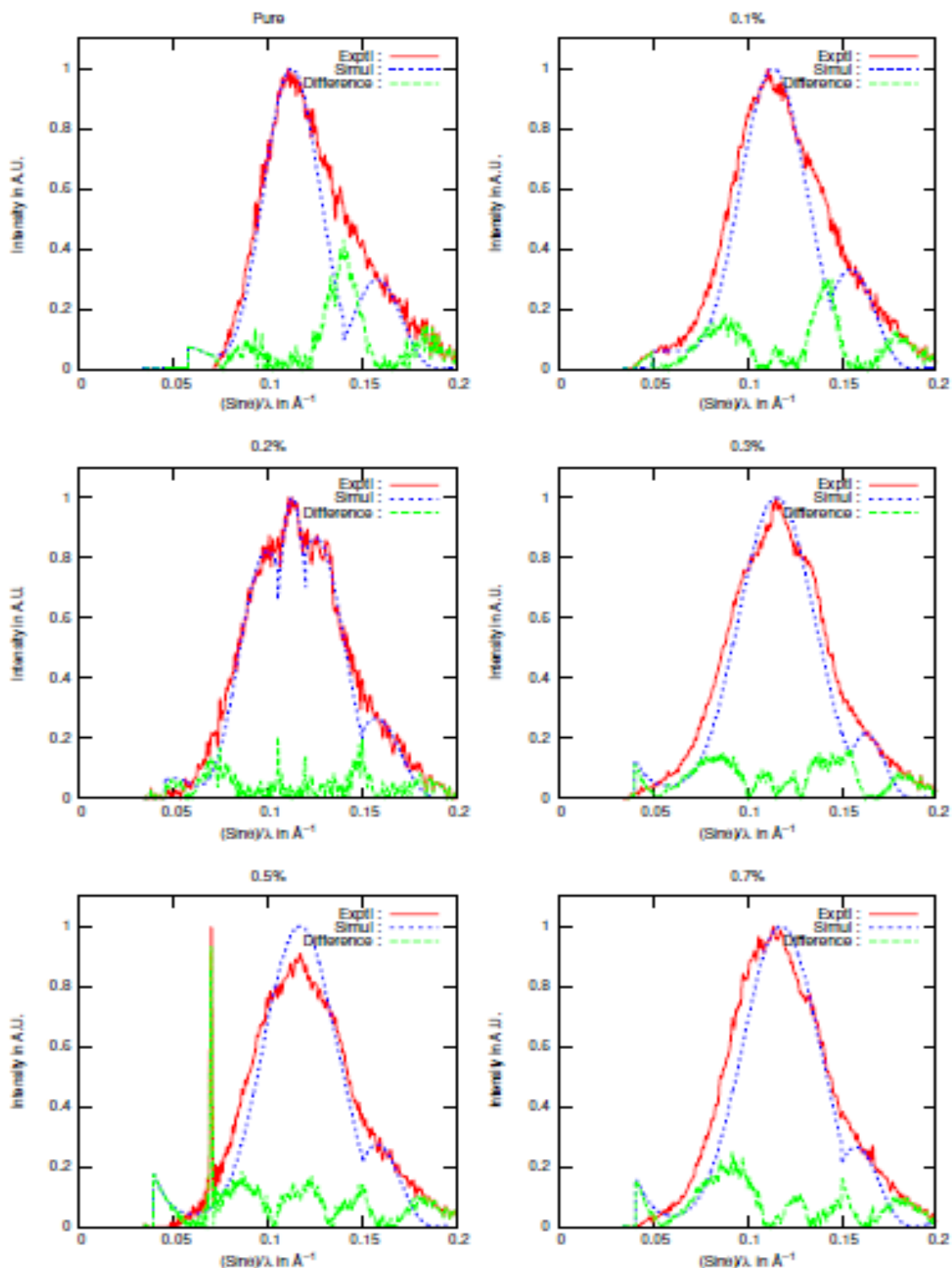


Figure 2(a): Simulated and experimental profiles for Epoxy – Nylon fabric laminates with 0.1 to 0.3 phr and 0.7 phr

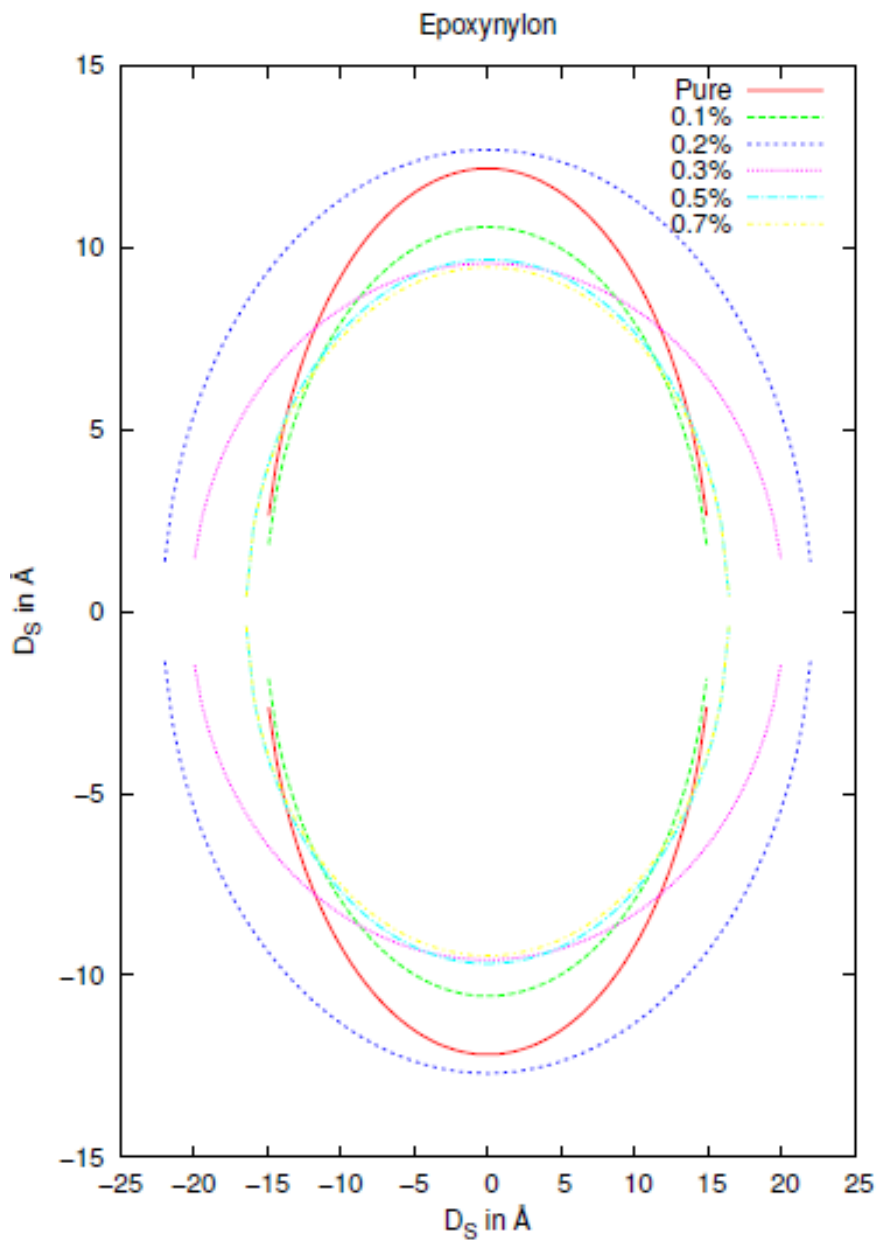


Figure 3: Variation of crystallite shape ellipsoid for Epoxy – Nylon fabric laminates with 0.1 to 0.7 phr

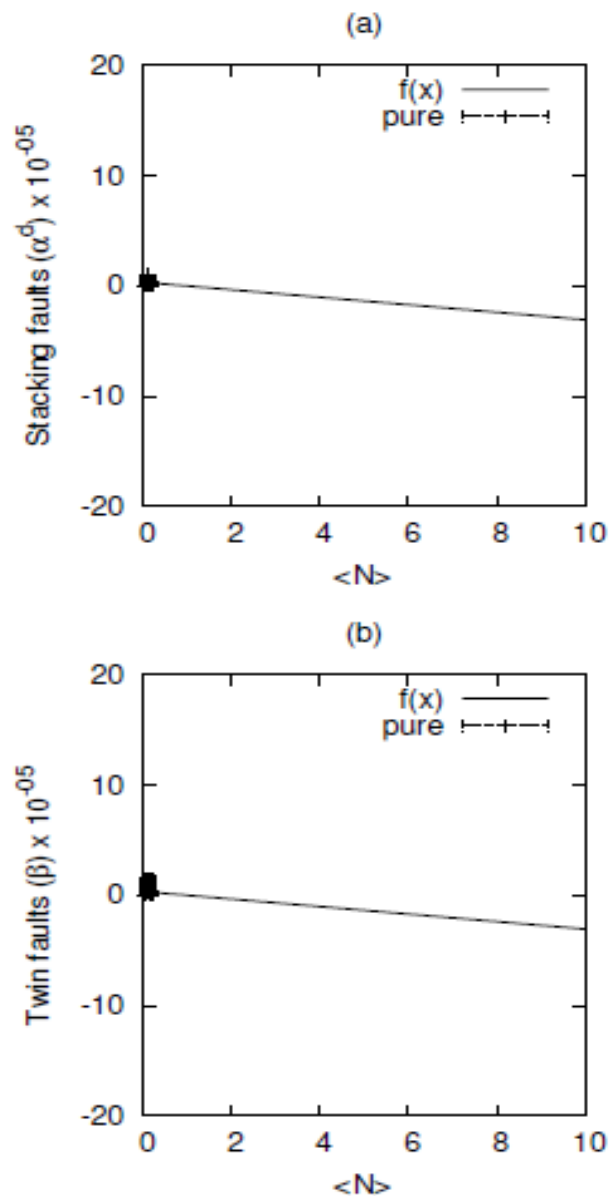


Figure 4: Stacking (a) and Twin faults (b) for Pure Epoxy – Nylon fabric laminates

Table 1

Micro structural parameters and stacking faults for Epoxy nylon using exponential distribution function

Epoxy nylon	20	N	d(Å)	D(Å)	g(%)	$\alpha$	$\alpha^d$	$\beta$	Delta( $\Delta$ )	Crystallite area (Å <sup>2</sup> )
Pure	20.01	2.75	4.43	12.18	0	2.41	1.92E-7	2.91E-7	2.65E-3	185.8
	27.98	4.80	3.18	15.26	0	3.35	9.36E-6	1.56E-5		
0.1	19.88	2.37	4.46	10.57	0	5.43	2.34E-9	4.83E-8	2.26E-3	159.9
	27.61	4.70	3.22	15.13	0	3.49	6.83E-6	6.56E-6		
0.2	17.69	2.57	5.00	12.85	0	9.07	3.89E-5	6.48E-5	1.25E-3	280.4
	20.04	5.00	4.42	22.10	0	2.75	2.75E-5	2.78E-5		
	22.29	3.19	3.98	12.69	0	7.99	9.24E-6	2.26E-5		
	28.07	4.80	3.17	15.21	0	3.60	2.93E-5	3.16E-5		
0.3	20.56	2.22	4.31	9.568	0	6.20	8.65E-8	1.14E-7	1.81E-3	193.1
	29.09	6.60	3.06	20.19	0	1.65	3.74E-6	2.25E-6		
0.5	20.4	2.23	4.34	9.678	0	6.54	2.00E-7	2.88E-7	2.50E-3	159.0
	28.19	5.20	3.16	16.43	0	2.28	2.02E-7	3.04E-5		
0.7	20.54	2.19	4.32	9.460	0	8.95	1.18E-6	3.12E-8	2.12E-3	155.4
	28.13	5.20	3.16	16.43	0	3.20	1.23E-7	2.06E-7		

## REFERENCES

- [1]. Timoty D. Stark, Thomas A. Williamson, Hisham T. Eid, (1996) HDPE Geomembrane/Geotextile Interface Shear Strength, J. Geotech. Engg. 122(3), 197 – 203.
- [2]. Price D M, Reading M, Hammiche A, Pollock H M, Branch M G, (1999) Localized thermal analysis of a packaging film, *Thermochimica Acta*, 332 143 – 149.
- [3]. Jane Maria Faulstich de Paivaa, Sérgio Mayerc, Mirabel Cerqueira Rezendea, (2006) Comparison of Tensile Strength of Different Carbon Fabric Reinforced Epoxy Composites, *Materials Research*, 9(1), 83 – 89.
- [4]. Xiao G, Liu J, Che L H, Li Y G, (2011) Design of the LHAASO-KM2A  $\mu$  Detector prototypes, 32<sup>nd</sup> International Cosmic Ray Conference, Beijing.
- [5]. Schwartz MM, *Composite Materials: (1997) Properties, Nondestructive Testing, and Repair. v. 1*, New Jersey, USA. Prentice-Hall Inc.
- [6]. Pilato LA, Michno MJ, (1994) *Advanced Composite Materials*, Berlin, Germany. Springer Verlag Berlin Heidelberg.
- [7]. Paul Akangah, Shivalingappa Ligaiah, Kunigal Shivakumar, (2010) Effect of Nylon – 66 nano-fiber interleaving on impact damage resistance of epoxy/carbon fiber composite laminates, *Composite Structures*, 92 1432 – 1439.
- [8]. Penn L S, Wang, H. *Epoxy Resins in Peters ST. Handbook of Composites 2<sup>nd</sup> ed.*, Peters St, editor, Chapman & Hall, Great Britain; 1998.
- [9]. Shim SB, Seferis JC, Eom YS, Shim YT, (1997) Thermal characterization and comparison of structural prepregs with different cure temperatures, *Thermochimica Acta.*; 291(1 – 2) 73 – 79.
- [10]. Mittemeijer E J and Scardi P, (2003) *Diffraction Analysis of the Microstructure of Materials*, Springer Verlag, (Berlin, Heidelberg).
- [11]. Snyder R L, Fiala J and Bunge H J, (1999) *Defect and Microstructure Analysis by Diffraction*, Oxford University Press, Editors.

- [12]. Scardi P and Leoni M, (2006)*J. Appl. Cryst.*, 39, 24.  
[13]. Welberry T R and Butler B D, (1994)*J. Appl. Cryst.*, 27(3), 205.  
[14]. Warren B E and Averbach B L, (1950) *J. Appl. Phys.*, 21, 595.  
[15]. Longford J I, (1965)*Nature*(London), 207, 966.  
[16]. Longford J I,(1968)*J. Appl. Cryst.*, 1, 131.  
[17]. Ribarik G, Ungar T and Gubicza J,(2001)*J. Appl. Cryst.*, 34, 669.  
[18]. Dong Y H and Scardi P, (2000) *J. Appl. Cryst.*, 33, 184.  
[19]. Scardi P and Leoni M, (2002)*Acta. Cryst.*, A58, 190.  
[20]. Balzar D, Audebrand N, Daymond M R, Fitch A, Hewat A, Langford JI, Lebail A, Louer D, Masson O, McCowan C N, Popa N C, Stephens P W and Toby B M,(2004)*J. Appl. Cryst.*, 37, 911.  
[21]. Hall I H and Somashekar R, (1991)*J.Appl.Cryst.*, 24, 1051.  
[22]. Somashekar R, Hall I H and Carr P D, (1989)*J.Appl.Cryst.*, 22, 363.  
[23]. Th H de Keijser, Langford J I, Mittemeijer E J and Vogels A B P, (1982)*J. Appl. Cryst.*, 15,308.  
[24]. Scardi P and Leoni M, (2001) *Acta. Cryst.*, A57, 604.  
[25]. Pope N C and Balzar D, (2002) *J.Appl.Cryst.*, 35, 338.  
[26]. Balzar D, IUCr (2002)Newsletter, 28, 14.  
[27]. Divakara S, Madhu S and R Somashekar, (2009)*Pramana.J. Phys.*, 73(5), 927 – 938.  
[28]. Veltrop L, Delhez R, De Keijser Th H, Mittemeijer E J and Reefman D, (2000)*J. Appl. Cryst*, 33 296 – 306.  
[29]. Jagodzinski H, (1949) *Acta Cryst*, 2 201 – 207.

ISIP